Massachusetts Institute of Technology
Harvard Medical School
Brigham and Women's/Massachusetts General Hosp.
VA Boston Healthcare System

2.79J/3.96J/20.441/HST522J

SURFACE CHARACTERIZATION AND ANALYSIS

M. Spector, Ph.D.

10.7 SIZE AND TIME SCALES FOR BIOADHESION

Size Scale	Tissue Level	Mechanism of Bonding	Time Constant	Measurement(s)
mm-cm	Organ	Interference Fit Grouting Agent Tissue (Bone) Ingrowth Chemical Bonding	Weeks-Months-Years	Radiographic (qualitative) Mechanical Testing (quantitative)
mm	Tissue	Same	Weeks	Mechanical Testing Light Microscopy/Histology (qualitative) Scanning Electron Microscopy (qualitative and quantitative)
µm	Cell	Integrin	Days-Weeks	Histology Transmission Electron Microscopy (qual.)
nm	Protein GAG	Secondary Bonding Hydrophobic Interactions	Seconds-Minutes-Hours-Days	Immunohistochemisty (qual.) Adsorption Isotherm (quan.)
nm	Mineral crystallites	Epitaxy Ionic Bonding	Seconds-Minutes-Hours-Days	Transmission Electron Microscopy *In vitro* Precipitation (quan.)

10.6 BIOADHESION (TISSUE BONDING): PHYSICAL AND CHEMICAL MECHANISMS

1. Physical/Mechanical
   a. Entanglement of macromolecules (nm scale)
   b. Interdigitation of ECM with surface irregularities/porosity (µm scale)

2. Chemical
   a. Primary
      ionic
   b. Secondary
      1) hydrogen bonding
      2) van der Waals
   c. Hydrophobic Interactions

CHEMICAL BONDING

Primary

• Metallic	100 kcal/mol
• Covalent	200
• Ionic	10-20

Secondary

• van der Waals	1-2
• Hydrogen	3-7
• Hydrophobic Interactions	1-2

MATERIALS WITH PRIMARY ATOMIC BONDS

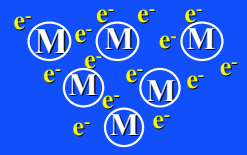

Metallic
(electron "glue" or "cloud")
-metals
-100 kcal/mol

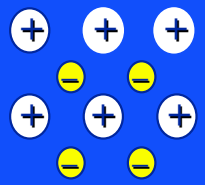

Ionic
(attraction of positive and negative ions)
-ceramics
-calcium phosphates
-10-20 kcal/mol

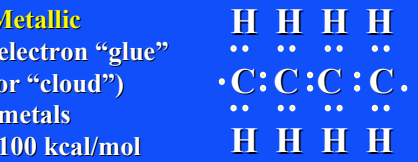

Covalent
(shared- pair electrons)
-polymers
-biological macromolec. (*e.g.*, proteins)
-200 kcal/mol

METALS

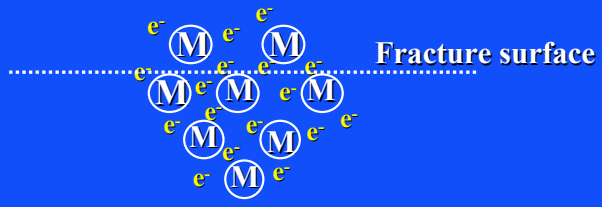

METAL SURFACE

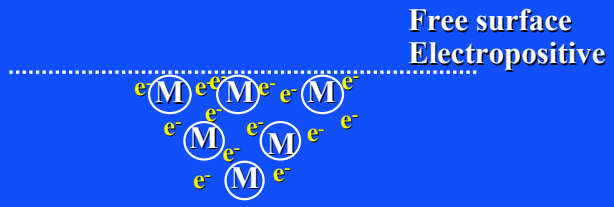

FORMATION OF METALLIC OXIDE

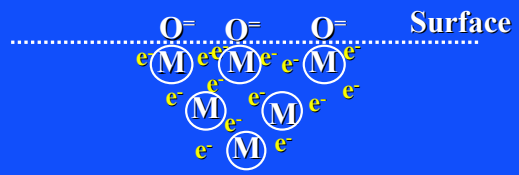

ORTHOPAEDIC METALS

	ADVANTAGES	DISADVANTAGES
Stainless Steel	Strength Ease of manuf. Availability	Potential for corrosion High mod. of elasticity
Cobalt-Chromium	Strength Rel. wear resist.	High mod. of elasticity
Titanium	Strength Low modulus Corrosion resist.	Poor wear resistance

METALS FOR TJA: PAST, PRESENT, AND FUTURE

1900-1940 1940-1960 1970 1980 1990 2000 2010

- Stainless Steel
- Cobalt-Chromium Alloy
- Titanium
- Oxinium

Oxinium® (Smith &Nephew Orthopaedics; oxidized zirconium) is the first new metal alloy in orthopaedic surgery in 30 years.

METALS FOR TJA: PAST, PRESENT, AND FUTURE

1900-1940 1940-1960 1970 1980 1990 2000 2010

- Stainless Steel
- Cobalt-Chromium Alloy
- Titanium
- Oxinium

Selection Criteria

- Inertness/Biocompatibility
- Strength
- Lower Modulus
- Scratch-resist.
- Lubricatious
- Non-Allergen.

ORTHOPAEDIC METALS

	ADVANTAGES	DISADVANTAGES
Stainless Steel	Strength Ease of manuf. Availability	Potential for corrosion High mod. of elasticity
Cobalt-Chromium	Strength Rel. wear resist.	High mod. of elasticity
Titanium	Strength Low modulus Corrosion resist.	Poor wear resistance
Oxinium	Scratch-resist. Low modulus	?

Composition of Orthopaedic Metals

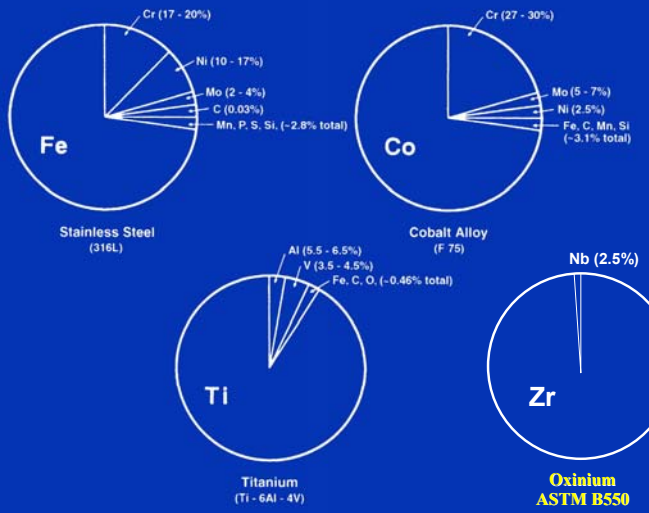

How is the Ceramic Surface Produced on Oxinium?: Oxidation Process

- Wrought zirconium alloy device is heated in air.
- Metal transforms as oxide grows; not a coating.
- Zirconium Oxide (Zirconia ceramic) is ~5 μm thick.

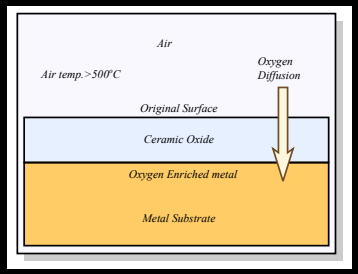

Figure by MIT OpenCourseWare.

G. Hunter, S&N

Co-Cr ALLOY VERSUS Zr-Nb ALLOY: THICKNESS OF THE OXIDE

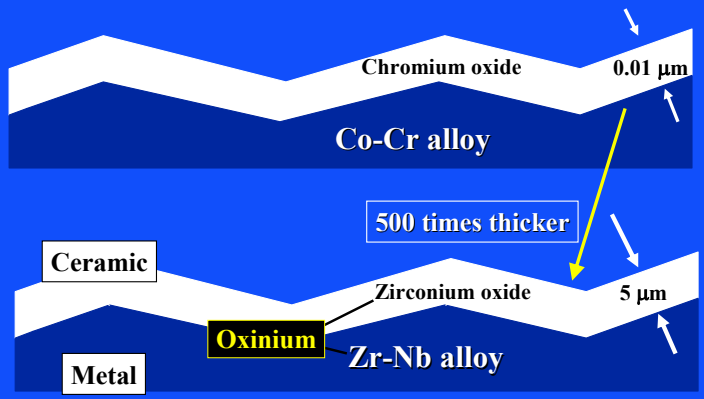

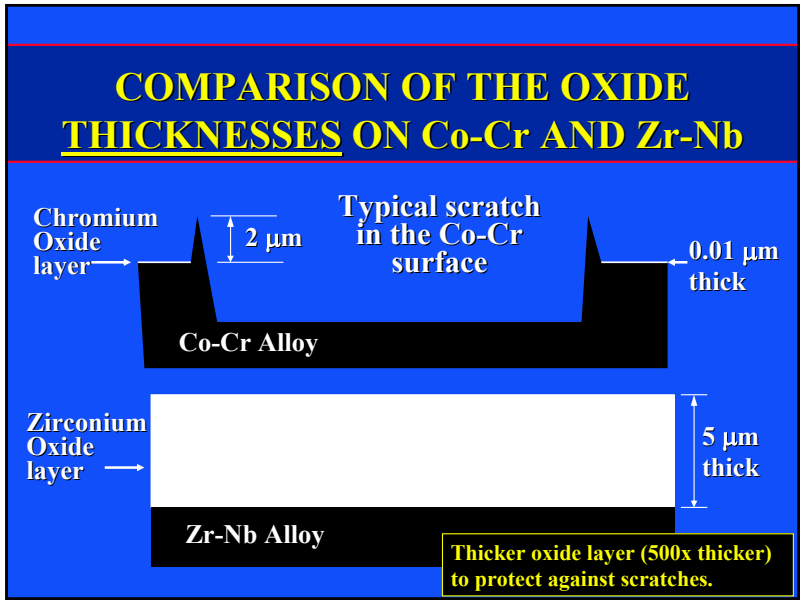

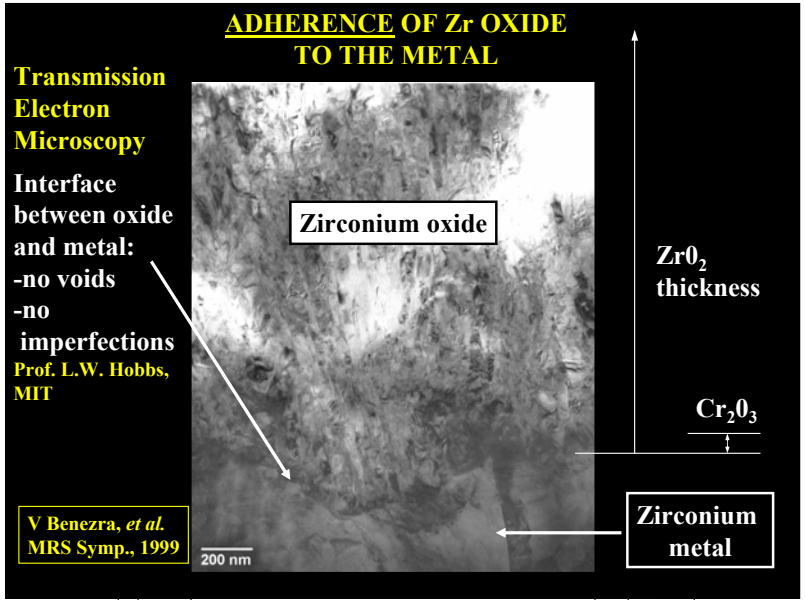

Source: Benezra V., M. Spector et al. "Microstructuralinvestigation of the oxide scale on Zr-2.5 Nb and its interface with the alloy substrate." In: Biomedical Materials -- Drug Delivery, Implants and Tissue Engineering. Mat. Res. Soc. Symp. Proc. Vol. 550 , 1999, pp. 337-342.

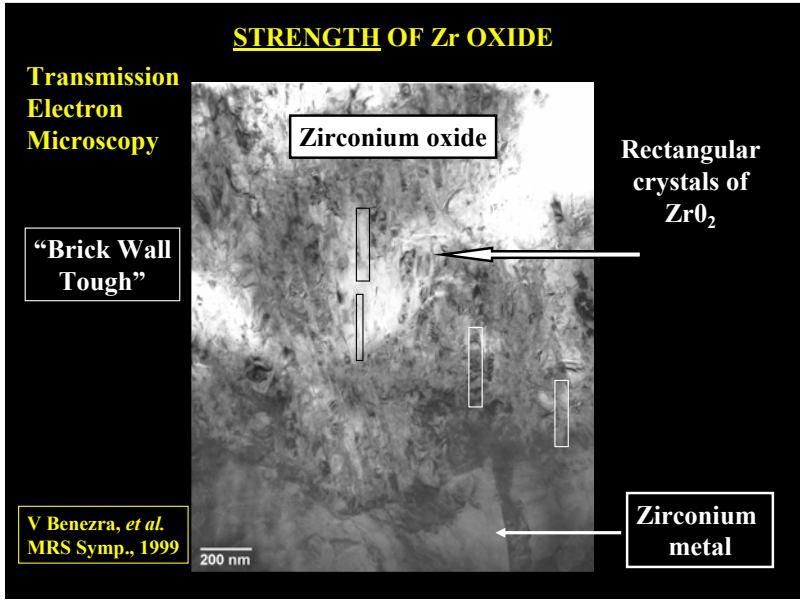

Source: Benezra V., M. Spector et al. "Microstructuralinvestigation of the oxide scale on Zr-2.5 Nb and its interface with the alloy substrate." In: Biomedical Materials -- Drug Delivery, Implants and Tissue Engineering. Mat. Res. Soc. Symp. Proc. Vol. 550 , 1999, pp. 337-342.

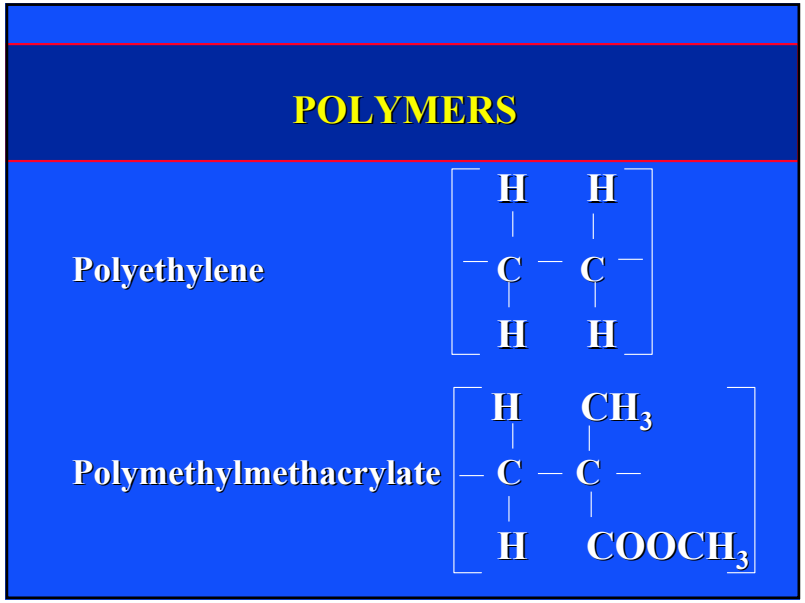

ULTRAHIGH MOLECULAR WEIGHT POLYETHYLENE

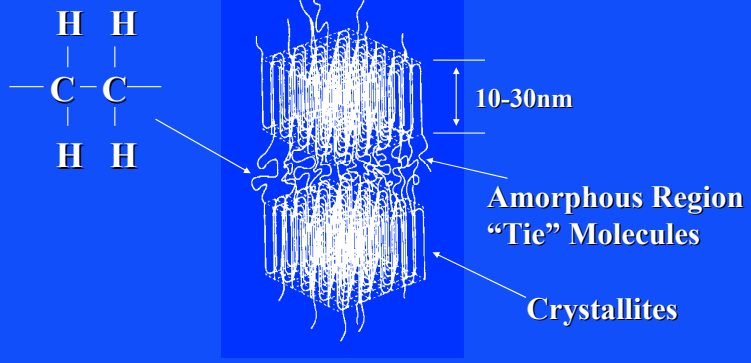

EFFECT OF GAMMA RADIATION ON PE: OXIDATION

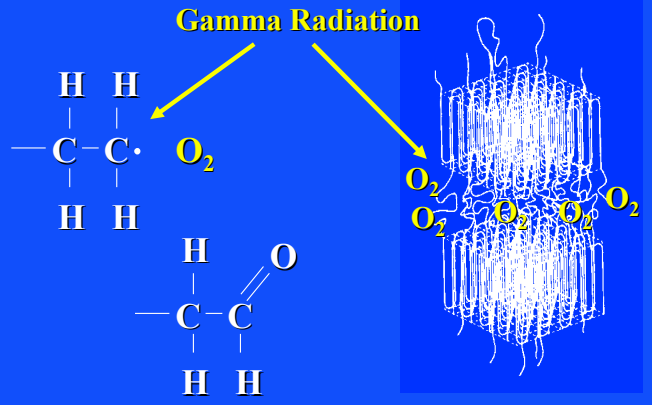

GAMMA-RADIATION INDUCED MODIFICATION OF POLYETHYLENE

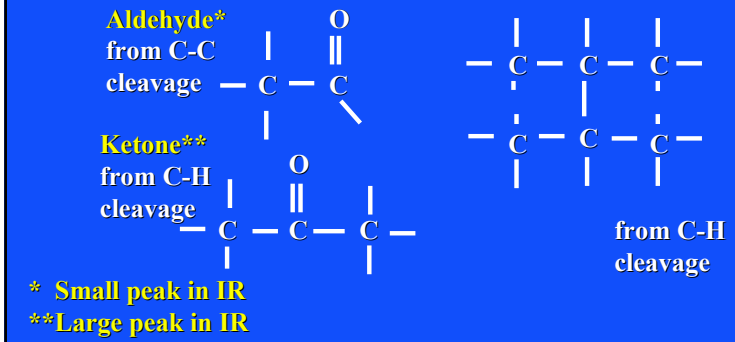

Slide removed due to copyright restrictions.
"Delamination and White Band: Impact of Gamma Sterilization in Air and Material Consolidation."
Sutula et al, AAOS 1995 Orlando

CHEMICAL BONDING

Primary

- Metallic — 100 kcal/mol
- Covalent — 200
- Ionic — 10-20

Secondary

- van der Waals — 1-2
- Hydrogen — 3-7
- Hydrophobic Interactions — 1-2

10.8 CHEMICAL AND PHYSICAL* BONDING (Nanometer Scale)

Biomaterial			Across Interface	Biological Molecules	
Classification	Bulk	Surface 0.1-5 nm		Intermolecular	Intramolecular
Metals	Metallic	Ionic	Hydrogen (3-7 kcal/mol)	Covalent	Covalent
Ceramics	Ionic/ Covalent	Ionic	van der Waals (1-2)	Ionic	Ionic
Polymers		CE	Ionic** (10-20)		Hydrogen
- Intramol	Covalent Ionic	Water (Hydrogel)	CE		Van der Waals
- Intermol	Covalent Ionic CE		Hydrophobic interactions (1-2)		Hydrophobic interactions

*Physical bonding - chain entanglement (CE), i.e., entanglement of polymer chains with biological macromolecules.

**Includes epitaxial crystal growth of biological mineral (e.g., bone mineral, apatite) on the biomaterial (e.g., synthetic hydroxyapatite or certain metal oxides).

10.5 SURFACE CHARACTERISTICS AND METHODS OF ANALYSIS

Scale of Features (Not Detection Depth of Penetration)	Characteristics	Method
Macroscopic (>10 μm)	Hydrophobicity	Contact angle (Critical surface tension from Zisman plot)
	Charge	Electrophoresis of particles (zeta potential)
	Topography	Light microscopy (LM) Scanning electron microscopy (SEM)
	Porosity	LM, SEM, Mercury intrusion porosimetry
	Water content	Drying/weighing
	Surface area	Gas adsorption methods
	Mechanical compliance	Mechanical testing (modulus of elasticity)

Microstructure		
(>0.2μm)	Particles on surface	Light microscopy/SEM
	Topography Profilometry (stylus pulled	Light microscopy, SEM, over surface)
	Crystallite Structure/Size	X-ray diffraction

Nanostructure		
>0.01μm (>10 nm)	Particles	SEM
	Topography	SEM, Profilometry
1-10 nm	Elemental composition analysis (EDX)	Energy dispersive x-ray
		Wavelength dispersive x-ray analysis (WDX)
		Electron spectroscopy for chemical analysis (ESCA, also referred to as x-ray photoelectron spectroscopy, XPS)
		Auger electron spectroscopy (AES)
		Secondary ion mass spectroscopy (SIMS)
	Molecules/Bonding (including depth profile, DP)	ESCA (DP)
		AES (DP)
		SIMS (DP)
		Infrared Spectroscopy (IR)
	Crystal structure	X-ray diffraction (XRD)

OBJECTIVES OF SURFACE ANALYSIS

- **Determine how the surface chemistry (and, therefore, properties) differs from the bulk (relative to the function of the material in the device, effects on the body, and response to effects on the body).**
- **Identify contaminants (*viz.*, with respect to effects of the material on the body).**
- **Identify chemical bonding possibilities for interactions with molecules in the biological milieu with respect to the effects of the material on the body (*viz.*, bioadhesion) and the body on the material.**

Image removed due to copyright restrictions.
Comparing visible length scales of unaided human eye, light microscope and electron microscope.

LIGHT MICROSCOPY

Image removed due to copyright restrictions.
Diagrams of diascopic and episcopic microscopes.

Slide removed due to copyright restrictions.
Description and diagram of compound light microscope.

LIGHT MICROSCOPY

The resolution (lateral) of the light microscope is:

$$D = \frac{0.611}{N \sin \alpha}$$

D = Smallest lateral dimension that can be resolved

N = Refractive index of medium surrounding the specimen (*i.e.*, air, 1.0, or oil, 1.5)

α = Angular aperture = $^1/_2$ angle of cone of light entering the objective lens from the specimen (depends on the width of the objective lens and distance from the specimen) -- increased by moving lens close to the specimen

N sin α = Numerical aperture

LIGHT MICROSCOPY

N sin α = Numerical aperture

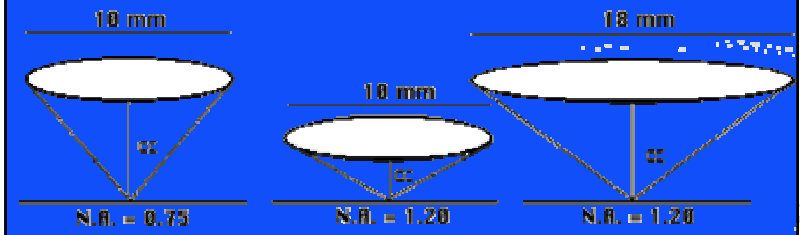

LIGHT MICROSCOPY

For specimens in air viewed by visible light:

N = 1.0

λ = 450 nm

D = 292 (0.3 μm)

For specimens in oil

D =200 nm (0.2 μm)

For ultraviolet light λ = 200 nm

D is approximately 1/2 λ

LIGHT MICROSCOPY

Another important parameter is depth of focus:

Magnification	Depth of Focus
10X	0.1 mm
100X	1 mm

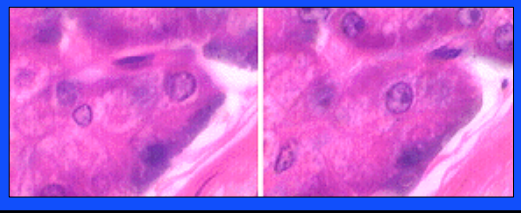

Types of Microscopy

Microscope	Incident Radiation	λ	Resolution (nm)	Depth of Penetration	Depth of Focus
Visible light	Light	450 nm	200	-	1 μm @ 100X
Ultraviolet light	UV	200 nm	100	-	
Electron [1]	e^-	0.005 (at 50 kV)			
Scanning [2]			2	1 μm	1 mm @ 100X
Transmission [3]			0.2	0.1 μm (thickness of section)	

1. **Specimen exposed to high vacuum**
2. **Specimen must have a conducting surface or the use of an "environmental" SEM to prevent "charging"**
3. **Ultra-thin sections (< 100 nm) are required**

Slide removed due to copyright restrictions.
Schematic diagram of electron microscope.

Slide removed due to copyright restrictions.
Interaction with Matter: Secondary electrons interact with topography
Back scatter electrons interact with composition
X-rays interact with chemistry

Slide removed due to copyright restrictions.
Photos of electron microscope equipment: detectors for secondary and back scatter electrons, and x-rays

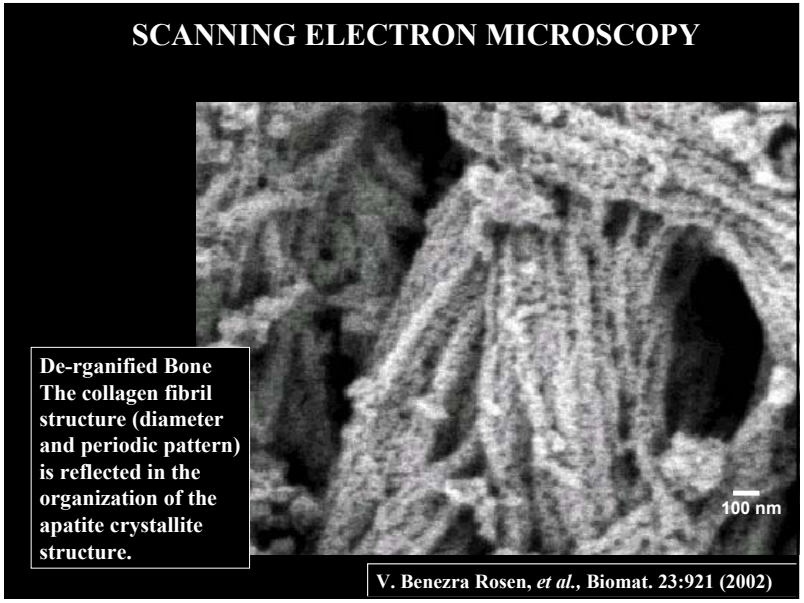

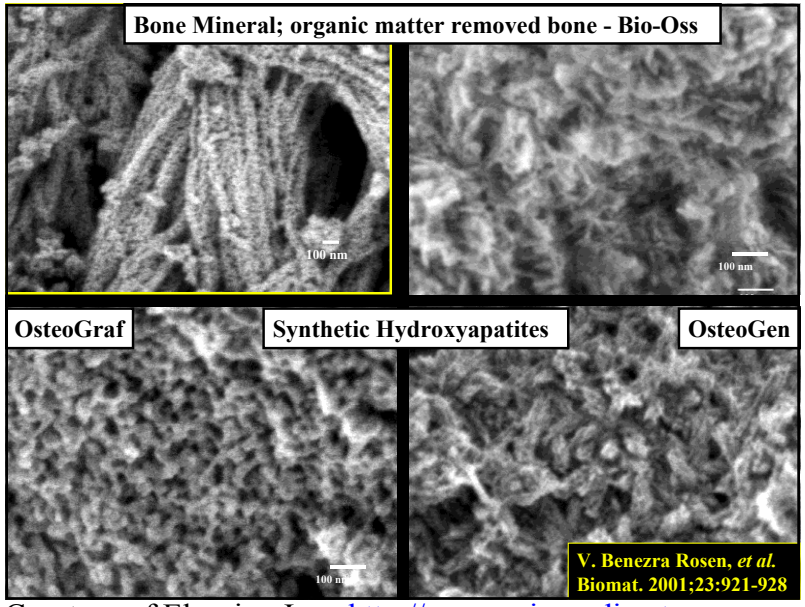

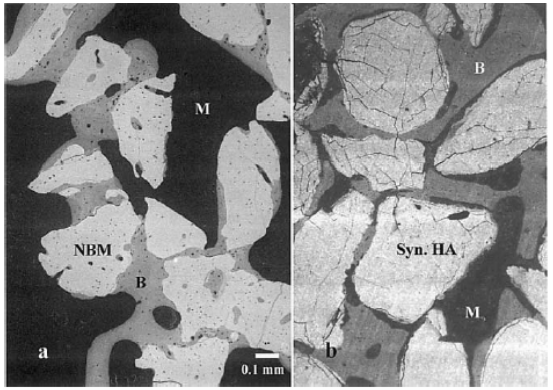

Fig. 4. (a) Backscattered electron image of NBM particles filling an implant site 26 weeks post-operatively. The whitish features are the NBM particles and the gray features the bone (B). The black regions are the marrow (M). (b) BEI of synthetic HA particles in a defect after 26 weeks showing the interconnectivity of the rabbit bone and the synthetic HA particles.

T. Orr, et al., Biomat 22:1953 (2001)

Slide removed due to copyright restrictions.
Schematic diagram of transmission electron microscope.

Lee DD and Glimcher M, J. Mol. Bio. 217:487, 1991
Lee DD and Glimcher M,. Conn. Tiss. Res. 21:247, 1989

TRANSMISION ELECTRON MICROSCOPY OF BONE

Images removed due to copyright restrictions.

M. Spector, J Microscopy 1975;103:55

60 nm

Transmission Electron Microscopy bONE

Two images removed due to copyright restrictions.
See Fig 4b and c in Benezra Rosen, V., et al. *Biomat*. 23:921 (2002).

Whole bone

- **Bovine bone from which all the organic matter was removed; anorganic bovine bone; Bio-Oss.**
- **The crystalline architecture is retained even after removing the organic (collagen) template.**

V. Benezra Rosen, *et al.*, Biomat. 23:921 (2002)

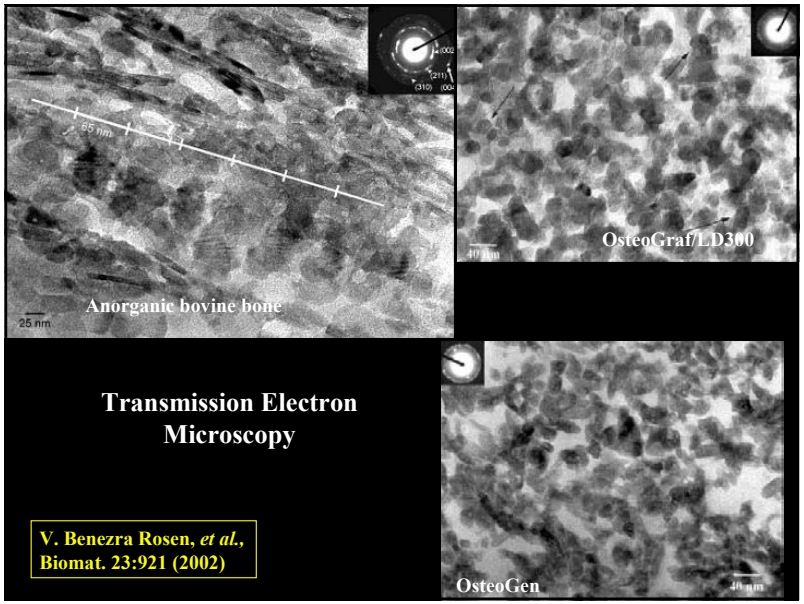

Courtesy of Elsevier, Inc., http://www.sciencedirect.com.
Used with permission.

Scanning Tunneling Microscopy

Schematic diagram removed due to copyright restrictions.

"Surf. Prop. of Biomat." in Biomat. Sci. Eds., B.D. Ratner, *et al.*, Academic Press, San Diego, CA, 1996

Diffraction Methods

- **Based on the principle that a monochromatic wave impinging on a regularly arrayed structure (*e.g.*, a crystal) will be diffracted at specific angles only, related to the spacing between the features in the array (*e.g.*, molecules).**
  - **The wavelength of radiation needs to be on the order of (or less than) the spacing to be detected.**
- **The diffraction pattern is a unique identifying feature of the material.**

Diffraction from a grating

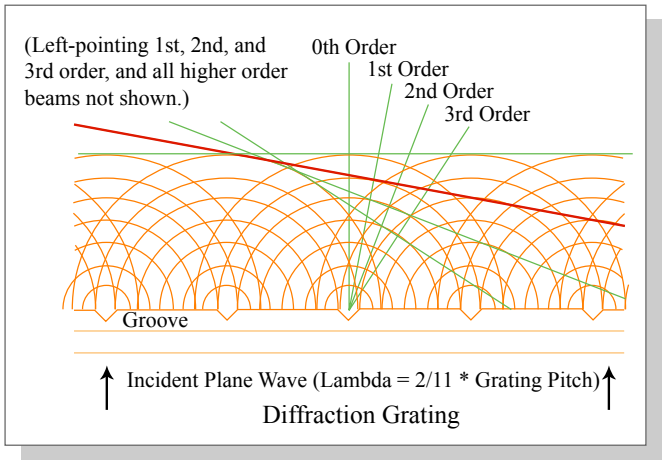

Figure by MIT OpenCourseWare.

X-RAY DIFFRACTION

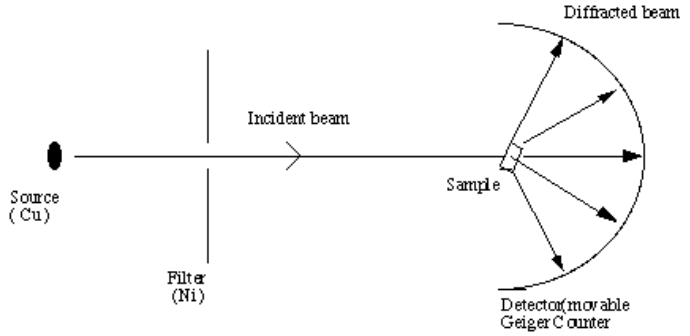

Bragg's Law

$$n\lambda = 2d \sin\theta$$

$$d = \frac{n\lambda}{2 \sin\theta}$$

n = integer indicating which multiple of the diffracted wave is being considered
λ = wavelength of radiation
d = spacing between features in the structure (*e.g.*, spacing between molecules in a crystal)
θ = the angle between incident and diffracted waves.

Width of peaks related to the crystallite size; narrower peak, larger crystallite

Photo and pair of graphs (natural bone mineral and synthetic hydroxyapatite) removed due to copyright restrictions.

CRYSTALLOGRAPHIC ANALYSIS (Powder X-ray Diffraction)

Sample	Structural Identification	Crystallinity	Crystallite Size: Peak	Size
Anorganic Bone	HA: >99.8% Non HA Ca-P: <0.2%*	88%	(002)	39 nm
Synthetic HA	HA	98%	(002)	90 nm

* Trace detection of α- and β-TCP, $Ca_2P_2O_7$ and CaO was observed however insufficient quantity of material existed for confident quantitative assessment.

START HERE

Types of Diffraction

Type of Diffraction	Radiation	λ
Optical	Laser light	400 nm
X- ray	X-ray	0.154 nm (for copper)
Electron	e^-	0.005 nm at 50 kV

Depth analyzed for x-ray diffraction (i.e., depth of penetration of the x-ray beam) is 1-10 μm.

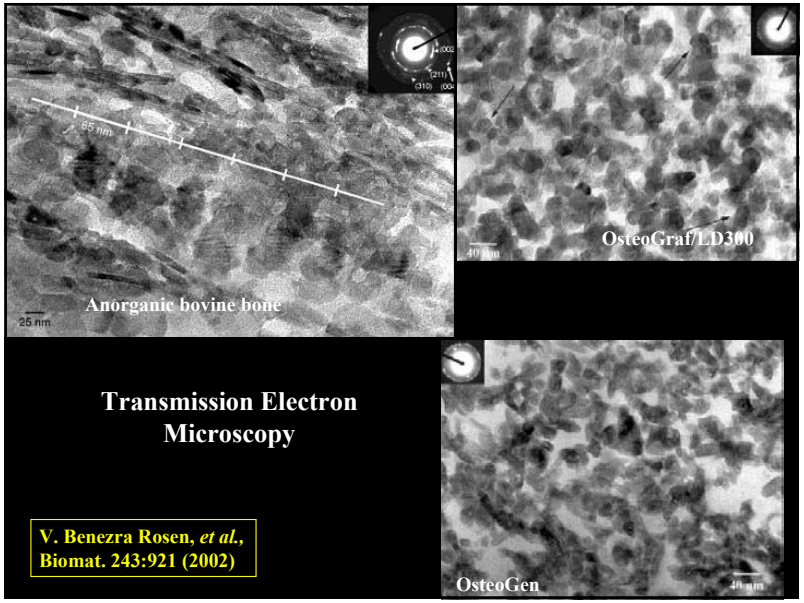

Transmission Electron Microscopy

V. Benezra Rosen, *et al.*, Biomat. 243:921 (2002)

Table 1 (Common Methods of Characterizing Biomaterials Surfaces) from Ratner removed due to copyright restrictions.
[Preview in Google Books]

"Surf. Prop. of Biomat." in Biomat. Sci. Eds., B.D. Ratner, *et al.*, Academic Press, San Diego, CA, 1996

Contact Angle and Critical Surface Tension

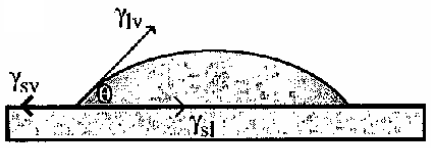

(included angle) = 0: complete wetting
0<θ<90°: partial wetting
θ>90°: nonwetting

Characterize a surface based on its critical surface tension, γ_{sv}.

At Equilibrium, ∑ surface tensions = 0

$\gamma_{sv}-\gamma_{sl}-\gamma_{lv}\cos\theta = 0$

$\gamma_{sv}-\gamma_{sl} = \gamma_{lv}\cos\theta$ Young's equation

Cannot solve for γ_{sv} because there are 2 unknowns, γ_{sl} and γ_{sv}

The experimental method employed to approximate γ_{sv} involves asking the question:
What is the surface tension of a liquid that would completely wet the solid surface?

Contact Angle Zisman Plot

Graph from Ratner removed due to copyright restrictions.

"Surf. Prop. of Biomat." in Biomat. Sci. Eds., B.D. Ratner, *et al.*, Academic Press, San Diego, CA, 1996

Table 2 (Critical Surface Tension Values for Common Polymers) from Ratner removed due to copyright restrictions.

"Surf. Prop. of Biomat."in Biomat. Sci.Eds., B.D. Ratner, et al., Academic Press, San Diego, CA, 1996

Contact Angle Assumptions

- **Equilibrium between the liquid droplet and solid surface has been reached (*i.e.*, no absorption of liquid by the solid and no leaking of substances from the solid).**
  - **If this assumption cannot be met then the "advancing angle" can be measured to determine the contact angle of the liquid with the dry surface and "receding angle" measured to determine the contact angle with the water absorbed surface.**
  - **An alternative method is to measure the underwater (captive-air-bubble) contact angle that an air bubble makes with the immersed surface. This is particularly valuable for measuring surface that can switch from hydrophobic to hydrophilic depending on the environment.**

Methods for Measuring the Contact Angle

Figure 5 from Ratner removed due to copyright restrictions.

"Surf. Prop. of Biomat." in Biomat. Sci. Eds., B.D. Ratner, *et al*., Academic Press, San Diego, CA, 1996

Table 3 (Concerns in Contact Angle Measurement) from Ratner removed due to copyright restrictions.

"Surf. Prop. of Biomat."in Biomat. Sci.Eds., B.D. Ratner, et al., Academic Press, San Diego, CA, 1996

SURFACE ANALYSIS

Incident Beam

- **X-Ray**
  - **X-Ray Photoelectron Spectroscopy**
- **Electron**
  - **Energy Dispersive X-Ray Microanalysis**
  - **Auger Spectroscopy**
- **Ion Beam**
  - **Secondary Ion Mass Spectroscopy**
- **Infrared Radiation**
  - **Infrared Spectroscopy**

Auger Electron Spectroscopy

- **Energy analysis of Auger electrons emitted from a sample. electrons are produced as a result of ionizations in inner core shells under impact of an electron beam.**
- **Significant intensity occurs for Auger electrons emitted with energies up to 2500 eV and these typically have a characteristic range between 1.5 and about 10 atom layers (0.4 to 3 nm).**
- **AES is sensitive to about 1% of most elements except H and He in the outermost atom layer and, generally, some of the atom layers just below the surface.**
- **The excitation is by an electron beam with energies in the range 5 keV to 25 keV.**
- **These beams may be focused to spot sizes of < 12 nm in most modern instruments.**

X-ray Photoelectron Spectroscopy
Electron Spectroscopy for Chemical Analysis (ESCA)

- **Energy analysis of photoelectrons emitted from a sample generated from core level shells under impact by characteristic X-rays, usually Al or Mg Ka.**
- **Photoelectrons have energies up to 1500 eV and typically have a characteristic range between 3 and about 8 atom layers (1 to 3 nm).**
- **XPS has a similar sensitivity to AES.**
- **It is sensitive to about 1% of most elements except H and He in the outermost atom layer and, generally, some of the atom layers just below the surface.**
- **This allows the composition to be determined as a function of depth to 10 nm below the surface, non-destructively.**

Figure 7 from Ratner removed due to copyright restrictions.

Electron Spectroscopy for Chemical Analysis, ESCA or X-ray Photoelectron Spectroscopy, XPS

Figure 6 from Ratner removed due to copyright restrictions.

ESCA or XPS

Figure 8 from Ratner removed due to copyright restrictions.

4 C peaks: hydrocarbon, C singly bonded to O, C in amide-like environment, and C in acid or ester environments

Figure 9 from Ratner removed due to copyright restrictions.

SURFACE AND BULK ANALYSIS

Sample	Analysis for§	Composition Ca	P	O	C	Ca/P Ratio:†
Anorganic Bone	Bulk:	27	16	57	–	Bulk: 1.69
	Surface:	19	13	58	10	Surface: 1.46
Synthetic Hydroxyapatite	Bulk:	25	15	60	–	Bulk: 1.67
	Surface:	20	13	58	9	Surface: 1.54

§ : Analysis for:
Bulk Composition: Energy Dispersive X-ray Analysis (0-2 μm sampling depth)
Surface Composition: Electron Spectroscopy for Chemical Analysis (0-5 nm sampling depth).

† : The stoichiometric ratio of Ca/P for Hydroxyapatite ($Ca_{10}(PO_4)_6(OH)_2$) is 1.67.

Static Secondary Ion Mass Spectrometry

- **Mass analysis of positive or negative ions emitted from samples under impact of an energetic ion beam.**
- **Significant intensity can occur for ions with masses up to and beyond 1000 a.m.u. that originate mainly from the outermost molecular layer.**
- **The fragments observed in the spectrum reflect the precise molecular groups on the surface.**
- **This allows distinction and identification not possible by AES and XPS but only where suitable reference spectra are available.**
- **SSIMS has a very much higher sensitivity than AES or XPS, but quantification is much more complex since matrix effects are dominant.**

Infrared Spectroscopy
Attenuated Total Reflectance Mode

Figure 11 A from Ratner removed due to copyright restrictions.

"Surf. Prop. of Biomat." in Biomat. Sci. Eds., B.D. Ratner, *et al*., Academic Press, San Diego, CA, 1996

Infrared Spectroscopy
External Reflectance Mode

Figure 11 B from Ratner removed due to copyright restrictions.

"Surf. Prop. of Biomat." in Biomat. Sci. Eds., B.D. Ratner, *et al*., Academic Press, San Diego, CA, 1996

Infrared Spectroscopy
Diffuse Reflectance Mode

Figure 11 C from Ratner removed due to copyright restrictions.

"Surf. Prop. of Biomat." in Biomat. Sci. Eds., B.D. Ratner, *et al*., Academic Press, San Diego, CA, 1996

20.441J / 2.79J / 3.96J / HST.522J Biomaterials-Tissue Interactions
Fall 2009